Sensitivity Analysis Around A Circular Cylinder

UROP PROJECT

Joel Outschoorn 01197636 | Department of Aeronautics | 19/09/2019

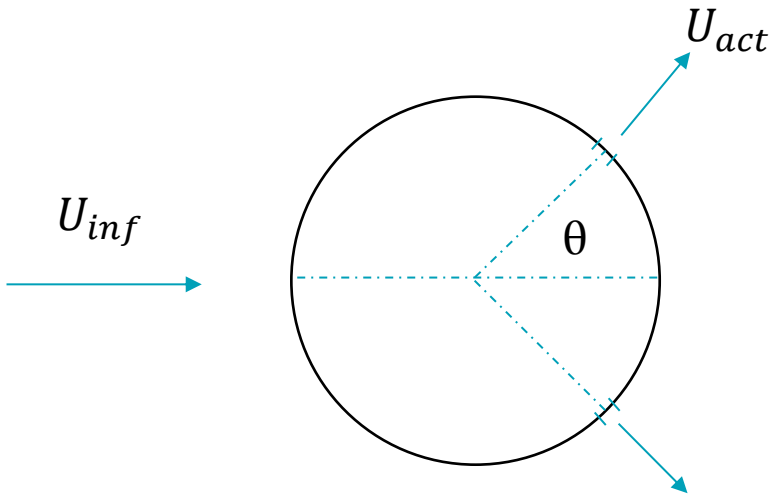

Abstract

This report outlines the procedure carried out to provide an approximation of the sensitivity of the drag on a 1 m diameter circular cylinder to flow actuation (blowing/sucking) on the cylinder surface. Actuators were located at 30-, 45-, 60- and 90- degrees from the horizontal (see above) with actuator velocities ranging from 0 to 1 m/s. The determined sensitivities can be seen in Tables 2 and 3 (pg. 9).

Nomenclature

θ	Angle of actuator from horizontal (degrees)
U_{act}	Actuation velocity (m/s)
U_{inf}	Free-stream velocity (m/s)
D	Generated drag on cylinder with no actuation (N)
D_{act}	Generated drag with actuation (N)
$\overline{D}$	$D - D_{act}$ (N)
C_d	2D drag coefficient with no actuation
$C_{d,act}$	2D drag coefficient with actuation
$\overline{C_d}$	$C_d - C_{d,act}$
Re	Reynolds number

1. Introduction and Motivations

The fundamental objective of this UROP project was to carry out sensitivity analysis around a circular cylinder. Through using localised actuation at the wall of the cylinder (blowing or suction), the long-term effects on the flow could be evaluated; in particular, the time average drag. Therefore, through running simulations with varying actuation velocities and actuator locations, sensitivity derivatives could be found. This could then be used as a comparison with other sophisticated methods to compute the sensitivities.

These methods involved adjoints, which prove to be more computational efficient of calculating sensitivities in comparison with finite differences. However, the adjoint method breaks down when the system is chaotic, for example the Navier-Stokes system. Thus, more complex approaches are required; Least-Square Shadowing (LSS) and Multiple-Shooting Shadowing (MSS) which will be discussed later.

The ultimate goal of carrying out sensitivity analysis of flow actuation on the cylinder is that the optimal actuation velocity at certain actuator locations can be determined to minimise time-average drag [1].

2. Literature Review

Commuting sensitivities of multidimensional problems is expensive through finite differences as it relies on the system to be solved through twice (once in the original state, then in the perturbed state). The adjoint method is applied through the first run hence it is more computationally efficient [2].

However, the adjoint method fails once the dynamic system is chaotic. The failure originating from what is known as the 'butterfly effect'. The problem could be overcome through exploiting the ergodic and hyperbolic properties of these systems which allowed the development of the LSS method [3]. It was found however, that this approach was computationally expensive. Hence the MSS method was developed, which is a computationally efficient version of the LSS approach. Details on the methodology can be found in [4]. The MSS method is still a new concept and has yet to be applied on the RANS equation. To ensure that reasonable values are reached from MSS a comparison would be useful.

3. CFD Analysis on Star-CCM+

The analysis of the circular cylinder was carried out on Star-CCM+. The main model configuration can be seen in Figure 1. Note that a symmetrical flow actuation was utilised to ensure no lift was generated as we were more interested in drag.

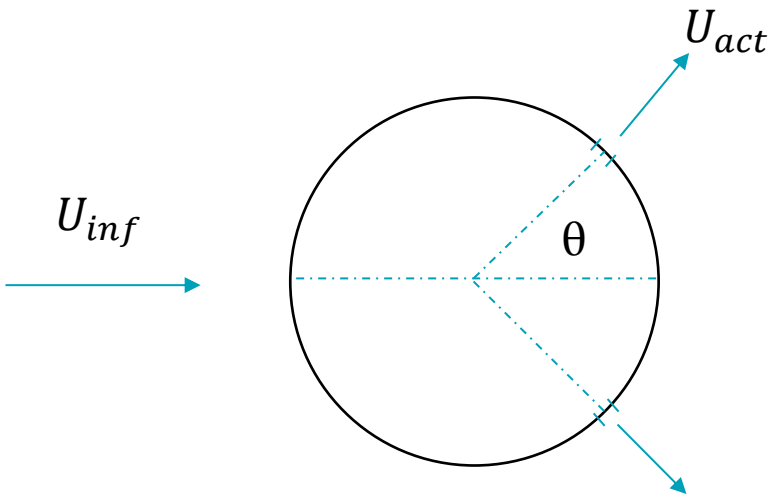

Figure 1: Model configuration on which simulations were run.

Various simulations were run with different actuation velocities (blowing and sucking) of 0.0, 0.2, 0.4, 0.8 and 1.0 m/s. Note that relatively small actuation velocities were applied to maximise the accuracy of the determined sensitivities. All velocities were run at different actuation locations, defined by θ. Angles of 30, 45, 60 and 90 degrees were analysed. Note that the actuator surfaces were modelled as straight 5mm panels.

The main parameters of the flow around the cylinder is tabulated below.

Table 1: Input parameters implemented into model.

Parameter	Value
U_{inf} (m/s)	50
Cylinder diameter (m)	1
Density (kg/m^3)	1.225
Dynamic viscosity (Pa.s)	1.8 x10^{-5}
Re	3.4 x10^6

Star-CCM+ uses both physics and mesh continua to approximately model the reality of the physical behaviour of the flow around the cylinder. The accuracy of the model depends on the mesh refinement and ensuring the correct physical conditions are implemented.

The physics model that was selected was a 2D steady, turbulent flow, implementing the k-Epsilon turbulence model (due to its popularity). The flow Mach number was 0.15, hence compressibility effects could be neglected. Segregated flow conditions were used rather than coupled flow simulations. These simulations compute the momentum and continuity components simultaneously. This uses a lot more RAM with no significant improvements in accuracy.

A trimmer mesh was employed, mesh refinement was applied around the cylinder walls and in the wake.

4. Results

The main outputs obtained were the drag (N) and the drag coefficient at each actuation velocity. These values were then normalised by subtracting each output from the output in the case with no flow actuation.

Plots of normalised drag, $\overline{D}$, against actuation velocity can be seen in Figures 2, 3, 6, 7 and plots of normalised drag coefficient, $\overline{C_d}$, against actuation velocity can be seen in Figures 4, 5, 8, 9. Note that Figures 2 to 5 represent the blowing actuation and Figures 6 to 9 represent the sucking actuation.

a. Blowing Actuation

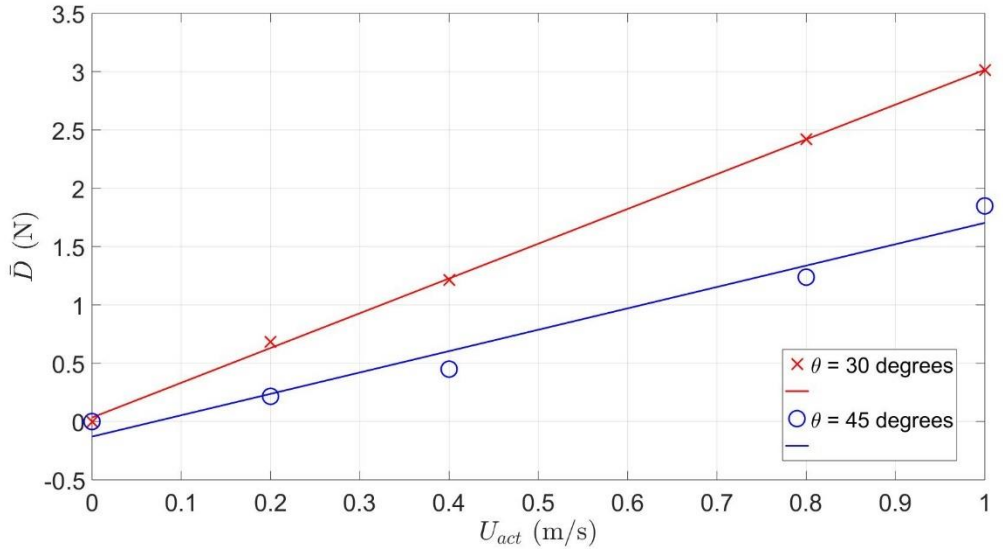

Figure 2: Drag versus actuation velocity for locations at 30 and 45 degrees from the horizontal.

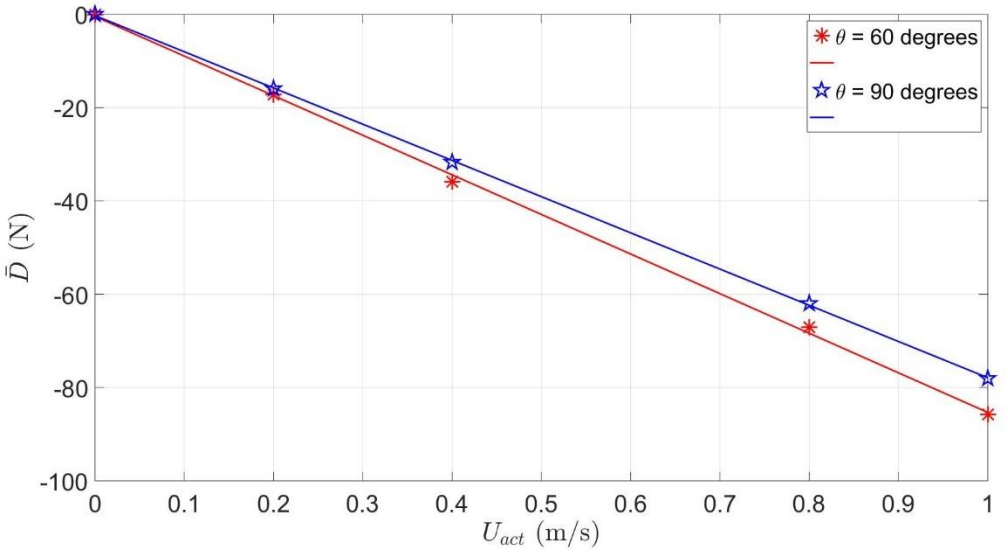

Figure 3: Drag versus actuation velocity for locations at 60 and 90 degrees from the horizontal.

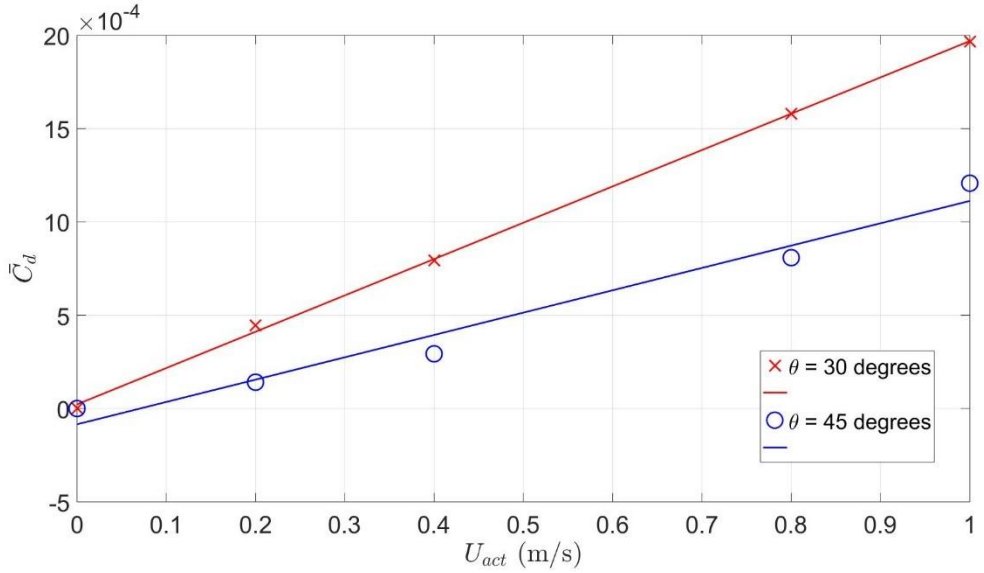

Figure 4: 2D drag coefficient versus actuation velocity for locations at 30 and 45 degrees from the horizontal.

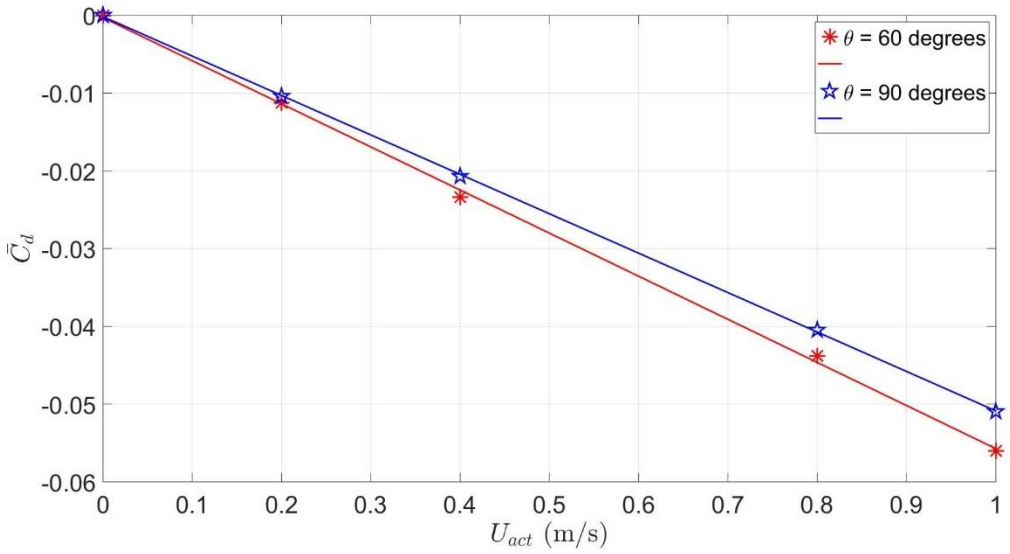

Figure 5: 2D drag coefficient versus actuation velocity for locations at 60 and 90 degrees from the horizontal.

b. Sucking Actuation

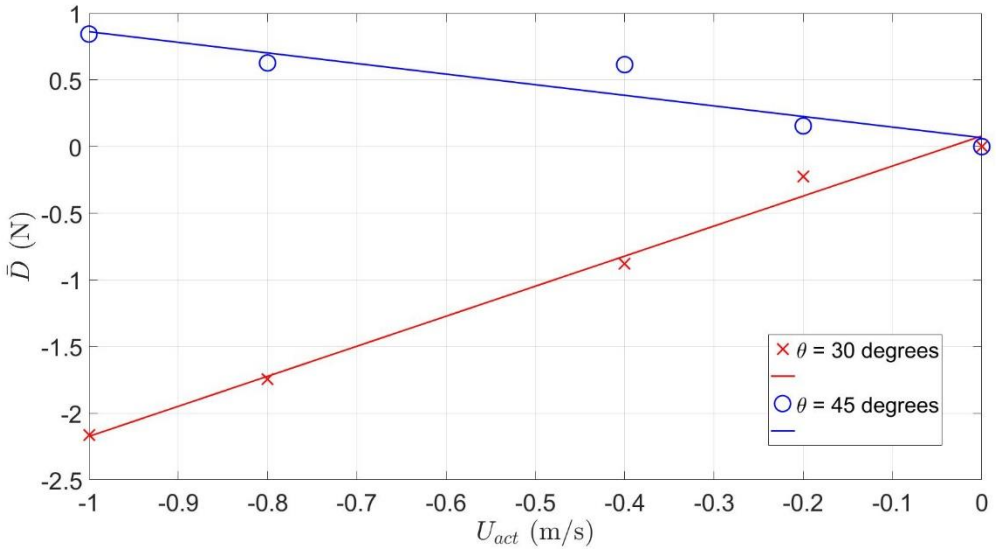

Figure 6: Drag versus actuation velocity for locations at 30 and 45 degrees from the horizontal.

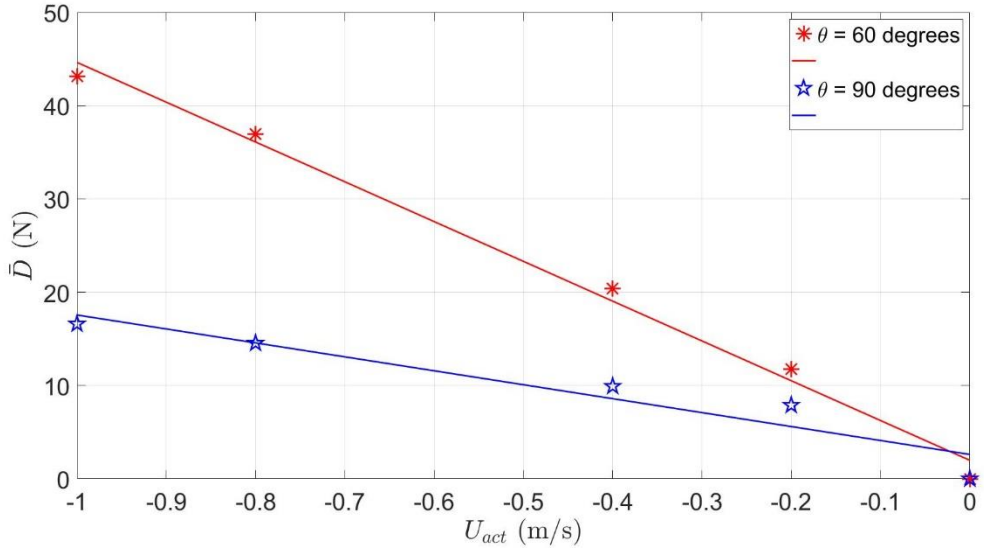

Figure 7: Drag versus actuation velocity for locations at 60 and 90 degrees from the horizontal.

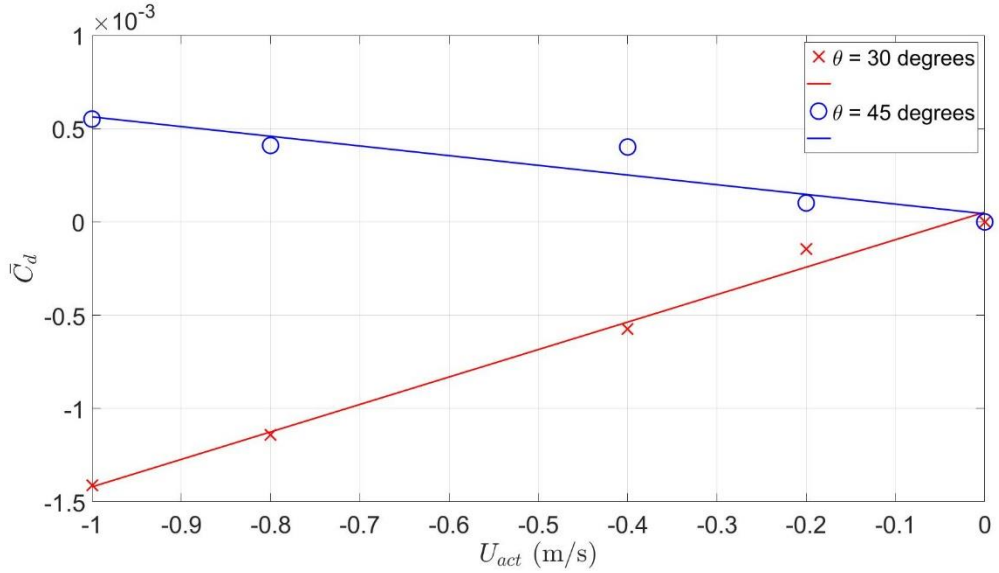

Figure 8: 2D drag coefficient versus actuation velocity for locations at 30 and 45 degrees from the horizontal.

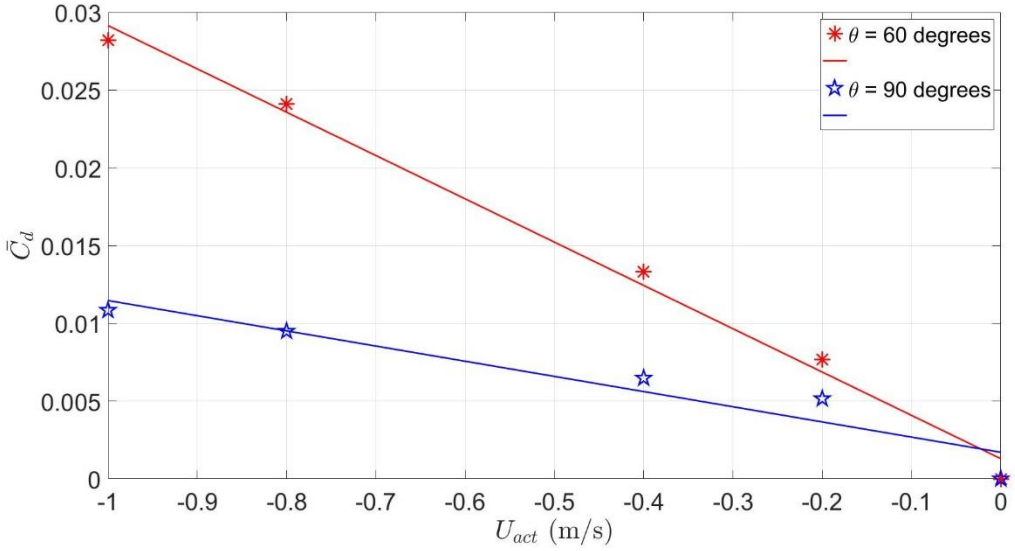

Figure 9: 2D drag coefficient versus actuation velocity for locations at 60 and 90 degrees from the horizontal.

A linear fit was implemented through the data points for each test case. The slopes of these fits were then determined and are tabulated below in Tables 2 and 3. These are approximations of the sensitivity derivatives which can be compared with those found through MSS discussed above.

Table 2: Sensitivities due to blowing actuation determined from slopes of Figures 2 to 5 above.

θ (degrees)	$\frac{d\bar{D}}{dU_{act}}$ **(Ns/m)**	$\frac{d\overline{C_d}}{dU_{act}}$ **(s/m)**
30	2.98	0.00195
45	1.56	0.00102
60	-84.9	-0.0554
90	-77.6	-0.0507

Table 3: Sensitivities due to sucking actuation determined from slopes of Figures 6 to 9 above.

θ (degrees)	$\frac{d\bar{D}}{dU_{act}}$ **(Ns/m)**	$\frac{d\overline{C_d}}{dU_{act}}$ **(s/m)**
30	2.25	0.00147
45	-0.795	-0.000519
60	-42.6	-0.0278
90	-14.9	-0.00976

5. Discussion

Through observing Figures 2 through 9, a linear fit seems to provide a good approximation of the correlation between the actuation velocity to generated drag.

Flow actuation at locations 60- and 90- degrees from the horizontal influence an increase in drag. Evaluating Table 2 and 3, the drag seems to be more sensitive to actuation at these locations as the sensitivities are relatively large in magnitude. As for the case of 30- and 45-degrees actuation, the drag is much less sensitivity to actuation velocity perturbations and flow actuation at these locations influence drag reduction. Furthermore, notice that the sensitivities for blowing actuation at 30- and 45- degrees are analogous (likewise with 60- and 90- degrees actuators).

A possible reason for the increased drag from actuators at 60- and 90- degrees is that at these locations, the airflow is still attached. Therefore, through introducing localised blowing the flow is disturbed which can encourage flow separation thus increasing drag. Furthermore, flow separation causes drag to increase significantly which could explain the large magnitudes of the sensitivity derivatives at these actuator locations.

Potential sources of error include defects arising from the mesh modelling. Despite convergence of the residuals the results may not be correct due to reduced mesh density. To limit this error a mesh convergence study was carried out to determine the minimum mesh size for which the outputs converge.

Moreover, the flow actuation was employed by small flat plates on the cylinder surface, hence the walls were not entirely round. This could have influenced errors in the outputs as the sharp change in the wall gradient would influence the local flow and is effectively the same principal as tripping the boundary layer. This notion was reinforced through evaluating the zero actuation drag. For a simple cylinder without these actuator surfaces generated 460N of drag. For a cylinder with the modelled actuators, in the same flow conditions, generated 525N of drag.

6. Conclusions

The main purpose of the analysis discussed above was to produce sensitivity derivative approximations to flow actuation on the surface of a circular cylinder. These outputs can be seen in Table 2. The values can then be used as a comparison with the newly developed MSS approach.

Further simulations could have been run on other actuator locations and wider range of actuator velocities. With the reassurance that these sensitivities are reasonable values (validation coming from the MSS outputs) then an optimisation problem can be developed. For certain actuator locations, the optimal flow actuation velocity can be determined to minimise drag (whether it be blowing or suction).

References

[1] Antony Jameson, Aerodynamic Shape Optimisation Using the Adjoint Method, Department of Aeronautics, Stanford University, February 2003.

[2] Andrew M. Bradley, PDE-constrained optimisation and the adjoint method, November 2010.

[3] Qiqi Wang, Least Square Shadowing sensitivity analysis of chaotic limit cycle oscillations, Aeronautics MIT, 2014.

[4] Patrick J. Blonigan, Qiqi Wang, Multiple shooting shadowing for sensitivity analysis of chaotic dynamical systems, Aeronautics MIT, 2018.

Appendix

A Flow Visualisation

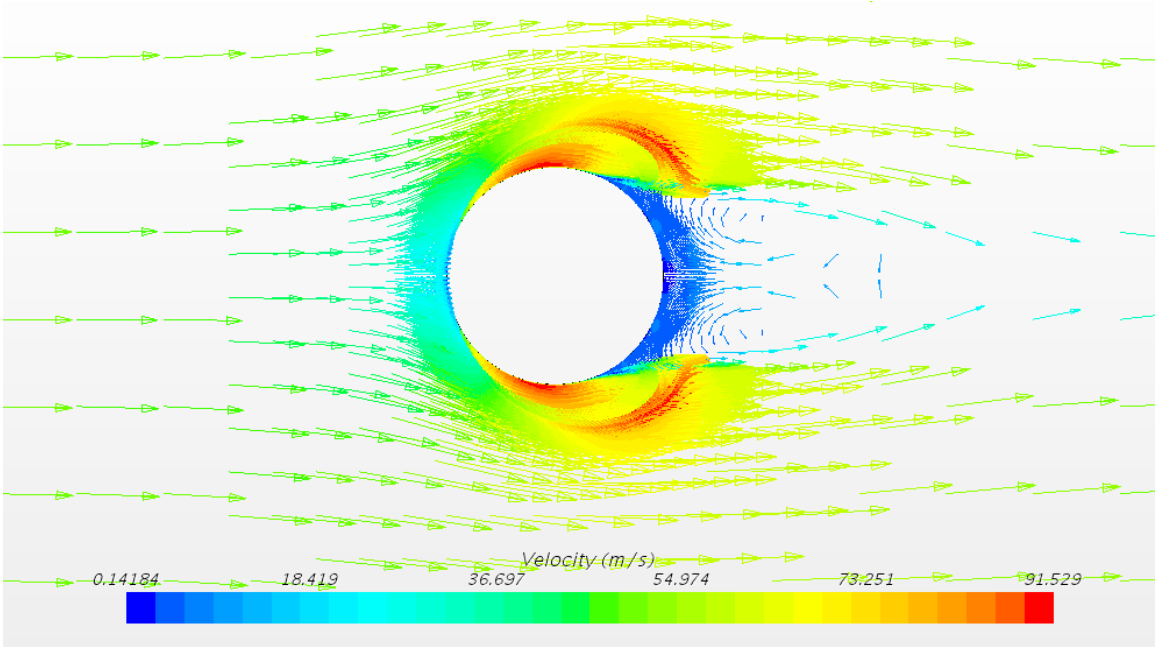

B Residual Plot

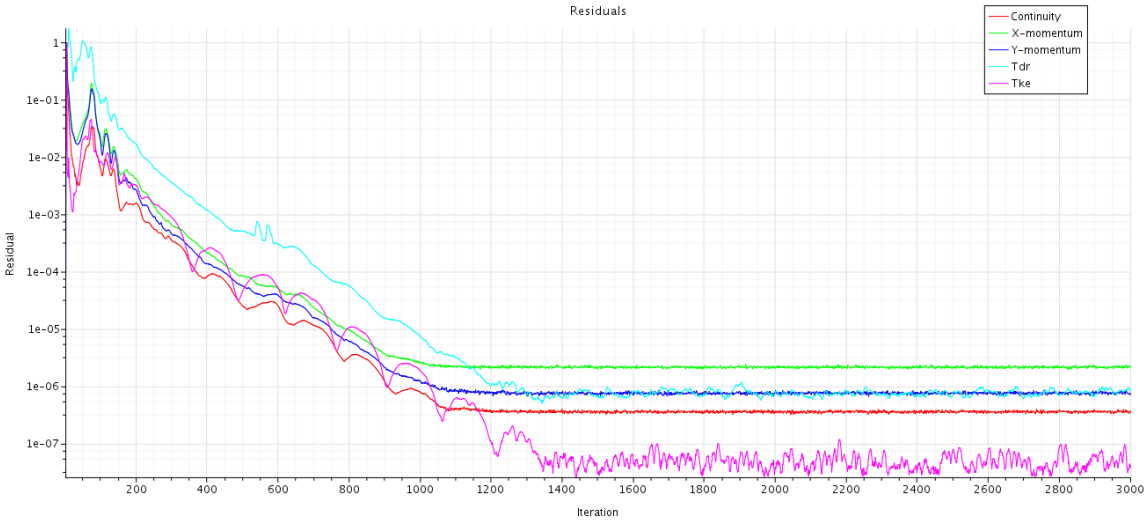

C Raw Data

Raw data can be found in attached Excel Spreadsheet.